

surements. Because of excessive viscous diffusion, the $k-\epsilon$ equations generated no leading-edge vortex and therefore compared poorly with the data. For a higher pitch rate, however, the $k-\epsilon$ solution agreed with the algebraic result. When $M_\infty = 0.4$, the $k-\epsilon$ model compared more favorably with the experiment than did the algebraic formulation.

Both the $k-\epsilon$ and Baldwin-Lomax solutions were fully turbulent from the airfoil leading edge. No attempt was made to simulate transition. This was unlike the experiment in which the transition location developed naturally and moved forward toward the leading edge as the angle of attack increased.

Neither model was entirely successful in predictive capability. Generally, the algebraic model produced less diffusion than was seen physically, whereas the $k-\epsilon$ equations produced more. These results clearly indicate that even for this restricted class of flows, the accuracy of simulation was highly case dependent and therefore evidences a need for turbulence models which better represent the fluid physics.

Acknowledgment

Computational resources for the work presented here were provided through the auspices of the Air Force Supercomputer Center, Eglin Air Force Base, Florida.

References

- ¹Baldwin, B. S., and Lomax, H., "Thin Layer Approximation and Algebraic Model for Separated Turbulent Flows," AIAA Paper 78-257, Huntsville, AL, Jan. 1978.
- ²Launder, B. E., and Sharma, B. I., "Application of the Energy-Dissipation Model of Turbulence to the Calculation of Flow Near a Spinning Disc," *Letters in Heat and Mass Transfer*, Vol. I, No. 2, 1974, pp. 131-138.
- ³Gerolymos, G. A., "Implicit Multiple-Grid Solutions of the Compressible Navier-Stokes Equations Using $k-\epsilon$ Turbulence Closure," *AIAA Journal*, Vol. 28, No. 10, 1990, pp. 1707-1717.
- ⁴Lorber, P. F., and Carta, F. O., "Unsteady Stall Penetration Experiments at High Reynolds Number," Air Force Office of Scientific Research, AFOSR TR-87-1202, East Hartford, CT, April 1987.
- ⁵Beam, R., and Warming, R., "An Implicit Factored Scheme for the Compressible Navier-Stokes Equations," *AIAA Journal*, Vol. 16, No. 4, 1978, pp. 393-402.
- ⁶Rizzetta, D. P., and Visbal, M. R., "Comparative Numerical Study of Two Turbulence Models for Airfoil Static and Dynamic Stall," AIAA Paper 92-4649, Hilton Head, SC, Aug. 1992.
- ⁷Visbal, M. R., "Dynamic Stall of a Constant-Rate Pitching Airfoil," *Journal of Aircraft*, Vol. 27, No. 4, 1990, pp. 400-407.

Intensified Array Camera Imaging of Solid Surface Combustion Aboard the NASA Learjet

Karen J. Weiland*

NASA Lewis Research Center, Cleveland, Ohio 44135

Introduction

FLAME spread over a paper surface in reduced gravity has received extensive study in drop tower facilities and has recently been observed in experiments aboard the Shuttle.¹⁻⁴ A common feature of flames produced in a reduced-gravity environ-

Presented as Paper 92-0240 at the AIAA 30th Aerospace Sciences Meeting, Reno, NV, Jan. 6-9, 1992; received March 26, 1992; revision received Aug. 24, 1992; accepted for publication Sept. 10, 1992. Copyright © 1992 by the American Institute of Aeronautics and Astronautics, Inc. No copyright is asserted in the United States under Title 17, U.S. Code. The U.S. Government has a royalty-free license to exercise all rights under the copyright claimed herein for Governmental purposes. All other rights are reserved by the copyright owner.

*Member Technical Staff, Space Experiments Division, 21000 Brookpark Road, MS 110-3.

ment at the investigated oxygen concentrations is a low-level blue luminosity which makes it difficult to record the flame shape and position on cine film. Thus, there is a need to improve the visualization system for these experimental studies.

Most reduced-gravity work on solid surface combustion has been performed at the NASA Lewis drop towers, which offer 2.2 or 5 s of microgravity, but have high g -level impacts measured from 30 to 100 g and more. The power for all equipment is usually supplied by batteries onboard the experimental package. Aircraft flying Keplerian trajectories offer a longer test time, 10 to 15 s, of reduced gravity and eliminate the shock loadings, but the g levels are not as low as in the drop towers. Residual g levels of ± 0.01 to 0.02 g are common and effects on flame behavior due to the g jitter also may be seen, but have not been quantified. Aircraft offer a more hospitable environment than the drop tower for the use of sensitive, delicate, and expensive instrumentation with regards to shock impact, power availability, and operator interaction.

This Note summarizes the results of six experiments conducted aboard the NASA Lewis Learjet. These flights were undertaken primarily to demonstrate the use of a commercial, intensified array camera to detect a flame from a solid surface combustion experiment in reduced gravity. The intensified array camera is able to detect light levels several orders of magnitude less than that detected by film or other nonintensified cameras. The remainder of the Note contains a description of the experimental apparatus and camera, the images obtained during the flights, and a brief comparison of the flame spread rates to previous drop tower measurements.

Experimental Approach

The combustion apparatus is described in more detail elsewhere.⁴ The combustion chamber is an engineering model of the solid surface combustion experiment first flown aboard STS-41 in October 1990. The paper samples are 100 mm \times 30 mm. Two types of paper are used: ashless filter paper of thickness 0.19 mm and laboratory wipers of thickness 0.076 mm. For each flight, one sample is loaded into a metal holder and placed in the 39-l chamber. The vertical orientation of the paper corresponds to the z direction. The x -, y -, and z -axis outputs from an accelerometer mounted

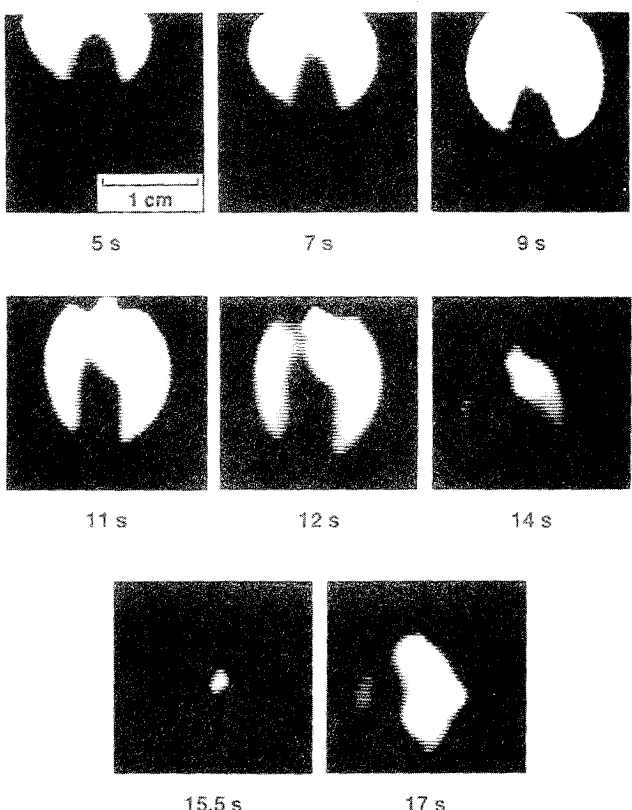


Fig. 1 Series of flame images for ashless filter paper burning in 21% oxygen.

near the center of gravity of the aircraft provide an indication of the g levels at the combustion chamber. The chamber is evacuated overnight to dry the paper and then filled with an oxygen/nitrogen mixture to 1 atm prior to flight. A current pulse through a wire woven onto the top end of the sample ignites the paper during a low-gravity trajectory.

The intensified array camera (Xybion ISG-207) is a charge injection device (CID). This camera contains a Generation II Red intensifier with a maximum luminous gain of 18,000. The photocathode has a spectral response range from 400 to 900 nm, and has a minimum faceplate sensitivity of 2×10^{-5} lux but at a signal-to-noise ratio of 1. The amplified, monochromatic image is transmitted by a bonded, tapered fiber optic to a CID array containing 242 V \times 388 H pixels. Ghosting of the images due to persistence of the P20 phosphor is not a problem. The camera body is ruggedized for durability in the presence of vibration or shock. A 28-mm focal length camera lens operating at $f/2$ is used to image the edge of the paper and the flame through a window in the chamber. The depth of focus is approximately 30 mm and the camera field-of-view is measured to be 105 mm V \times 140 mm H. The camera is operated nongated, i.e., an exposure time of 16.7 ms per video field. For one test, a narrowband interference filter centered at 431 nm is placed before the lens to reject emission from soot and char and transmit emission from the CH radical. The camera video output is recorded by a videocassette recorder and viewed on a monitor during the experiment. The automatic gain control is not used in the camera. The camera gain is varied manually by the experimenter by

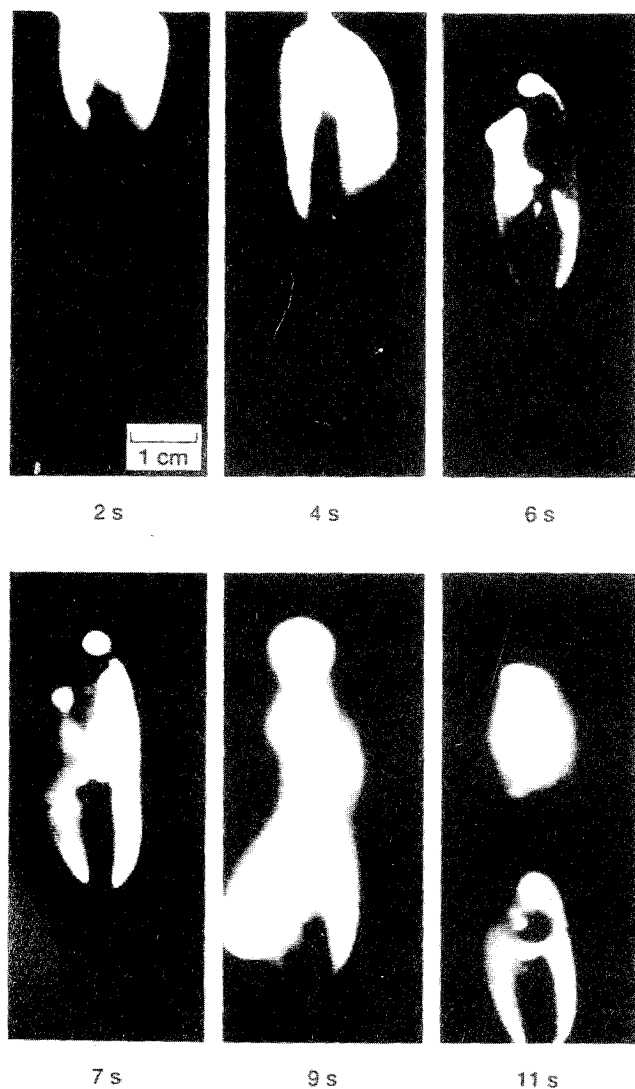


Fig. 2 Series of flame images for a laboratory wiper sample burning in 21% oxygen.

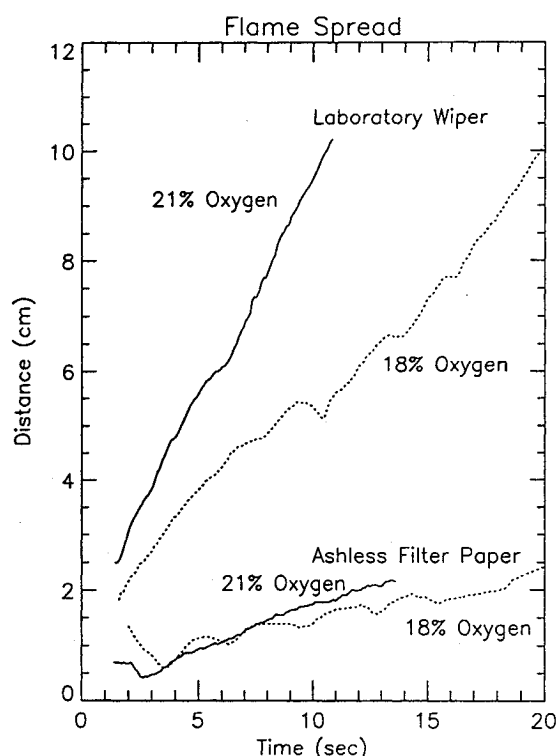


Fig. 3 Flame position vs time from ignition for ashless filter paper and laboratory wiper samples burning in 21% and 18% oxygen. The distance is a relative measurement.

adjusting the voltage level on the microchannel plate of the camera. A computer digitizes and records data on the plate voltage readout signal, which is converted into the microchannel plate voltage. (This data for two of the flights were not recorded, but the potentiometer positions during most of the experiment were noted.) This data is needed if the camera automatic brightness control limits the microchannel plate voltage to a value below what the experimenter has chosen. From this data, the camera gain may be determined by calibration. For a more complete description of the camera's performance compared to film, the reader is referred to Ref. 5.

The videotaped flame images are digitized frame by frame and electronically transferred to a workstation for analysis using commercial visual data analysis software. Flame positions at the leading edges are measured at every 0.1 s. Polaroid photographs of the images are taken from a monitor for display here.

Flame Images

The intensified array camera observes flames for both types of paper samples burning in 21 and 18% oxygen without being at its highest gain. The spread rates for the flames could be measured and are discussed in the next section. An image sequence from the ashless filter paper sample burning in 21% oxygen is shown in Fig. 1. The flame burns steadily for the first 10 s, but then diminishes in intensity and almost extinguishes at 16 s. When the aircraft begins its 2-g pullup, the flame flares brightly. The 18% oxygen, ashless filter paper flame, not shown here, also burns throughout the reduced-gravity period. The intensified array camera gains are at 18 and 72 for most of the time during these two experiments. Little detail is seen in the images, partially due to the limited resolution of the detection array, but also because the CID array may be saturated. The problem of how to set the gain to provide the correct exposure is evident. Currently, the experimenter manually sets the gain while observing the image on the video monitor, as the autogain of the camera tends to overexpose the flame when it is observed against a black background.

For the remaining four flights, faster burning laboratory wiper samples are used. A series of flame images for the laboratory wiper

sample burning in 21% oxygen is shown in Fig. 2. The flame burns the length of the sample in 11 s. The camera detects small glowing pieces shooting out from the flame and some of the char glowing and folding over into the flame. The width of the flame on each side of the paper changes during the burn. During this time, the lateral g level crosses from one direction to the other. The 18% oxygen, laboratory wiper flame, not shown here, burns to completion in the reduced-gravity period. The intensified array camera gains for these two flames are 72 and 1800. The flames would have been difficult to detect using film or conventional color CCD cameras. An additional test using 18% oxygen, with the narrowband interference filter, produced inconclusive results. Because the filter bandwidth of 1 nm is too narrow compared to the CH spectral bandwidth of 10–15 nm at flame temperatures, the image appears dim. The laboratory wiper sample in 15% oxygen appear to ignite but extinguishes quickly. No flame is detected after 5 s with the camera at its highest gain.

Flame Spread Rates

Measurements of the flame spread rates are useful for an order-of-magnitude comparison to other reduced-gravity measurements, although the induced flows due to buoyancy are not known. For each flame, the leading edge is specified to occur at a gray level chosen by eye, e.g., 60 out of 255, and its position is measured for each frame. The relative flame positions vs time from ignition for four tests are shown in Fig. 3. After the first few seconds of ignition and stabilization, the flames spread steadily over the paper samples.

The average flame spread rates for the ashless filter paper burning in 21% oxygen and 18% oxygen are 0.16 cm/s and 0.09 cm/s, respectively. The approximate z -axis g level for the 18% oxygen test oscillates between $\pm 0.02 g$. The flame position advances and retreats on a timescale of seconds and appears to correlate, as does the flame standoff, with positive and negative g levels. As the flame advances, the leading edge narrows and approaches the paper; as the flame retreats, the leading edge widens. Both flames move little during the reduced-gravity time and may be influenced by the presence of the ignitor. There is little data obtained in reduced gravity for this fuel with which to make a comparison. Some unpublished data, obtained in the NASA Lewis Zero Gravity facility, show that ashless filter paper samples burning in a 1 atm, 30% oxygen–70% nitrogen, quiescent environment have a spread rate of approximately 0.12 cm/s.⁶ The flame images are dim blue and difficult to analyze. The flame spread rate observed here for ashless filter paper in 21% oxygen is higher than that measured in the quiescent, 30% oxygen drop tower test, probably due to the induced buoyant flow from the residual g level.

The laboratory wiper samples burn faster than the ashless filter paper samples. The average flame spread rates for the laboratory wiper in 21% oxygen and 18% oxygen are 0.8 cm/s and 0.5 cm/s, respectively. Previous drop tower experiments using this fuel show a spread rate of 0.54 cm/s at the molar oxygen extinction limit of 21% for quiescent flame spread.² When a slow opposed flow or concurrent flow on the order of 5–7 cm/s is imposed, the flame spread rate increases above the quiescent flame spread rate.^{2,3} The flame spread rate for the laboratory wiper in 21% oxygen observed here is higher than the quiescent drop tower measurement, but is consistent with the presence of induced flows on the order of those studied in the forced-flow experiments in the drop tower. Likewise, the flame spread rate for a laboratory wiper in 18% oxygen observed here is similar to those measured using a slow opposed flow or concurrent flow in the drop tower.^{2,3}

Conclusions

An intensified array camera has successfully imaged weakly luminous flames spreading over thermally thin paper samples in a reduced-gravity environment aboard the NASA Learjet. The residual g level of the aircraft affects the flammability, flame shapes, and spread rates. The flammability and measured flame spread rates for the laboratory wipers in 21 and 18% oxygen for these “quiescent” aircraft experiments are similar to those obtained in

forced-flow drop tower experiments, suggesting substantial induced flows due to the residual g levels are present.

References

- ¹The Microgravity Combustion Group, “Microgravity Combustion Science: Progress, Plans, and Opportunities,” NASA TM-105410, April 1992, pp. 6–11.
- ²Olson, S. L., Ferkul, P. V., and Tien, J. S., “Near-limit Flame Spread over a Thin Solid Fuel in Microgravity,” *Twenty-Second Symposium (International) on Combustion*, Combustion Inst., Pittsburgh, PA, 1988, pp. 1213–1222.
- ³Grayson, G., Sacksteder, K. R., and Tien, J. S., “An Experimental Study of Low-Speed, Concurrent-Flow Flame Spread over a Thin Fuel,” Central States Meeting of the Combustion Inst., Nashville, TN, 1991.
- ⁴Vento, D. M., Zavesky, R. J., Sacksteder, K. R., and Altenkirch, R. A., “The Solid Surface Combustion Space Shuttle Experiment Hardware Description and Ground-Based Test Results,” AIAA Paper 89-0503, Jan. 1989; also NASA TM-101963.
- ⁵Weiland, K. J., “Intensified Array Camera Imaging of Solid Surface Combustion Aboard the NASA Learjet,” AIAA Paper 92-0240, Jan. 1992; also NASA TM-105361, 1992.
- ⁶Olson, S. L., private communication, NASA Lewis Research Center, Cleveland, OH, Nov. 1991.

Implicit Treatment of Diffusion Terms in Lower-Upper Algorithms

T. I-P. Shih* and E. Steinhorsson†

*Carnegie Mellon University,
Pittsburgh, Pennsylvania 15213*

and

W. J. Chyu‡

*NASA Ames Research Center,
Moffett Field, California 94035*

Introduction

THE lower-upper (LU) algorithm^{1,2} is a highly efficient method for obtaining numerical solutions to the “compressible” Euler and Navier-Stokes (N-S) equations. So far, when using the LU algorithm to analyze the N-S equations, the diffusion terms have usually been treated explicitly.^{3–6} This is because the LU algorithm factors according to the signs of eigenvalues associated with the Jacobians of the flux vectors, and such eigenvalues do not exist for the diffusion terms. When diffusion terms are treated explicitly, the robustness of the LU algorithm can be degraded. In fact for three-dimensional problems, numerical experiments have indicated that the LU algorithm can become unconditionally unstable if the residual is dominated by diffusion terms.⁶

In this Technical Note, a method is presented which allows diffusion terms to be treated implicitly in the LU algorithm in order that its good stability properties will not be impaired. The method presented generalizes the concept of LU factorization from that associated with the signs of eigenvalues to that associated with backward- and forward-difference operators without regard to eigenvalues.

Received May 11, 1992; revision received Oct. 13, 1992; accepted for publication Oct. 16, 1992. This paper is declared a work of the U.S. Government and is not subject to copyright protection in the United States.

*Associate Professor, Department of Mechanical Engineering. Member AIAA.

†Graduate Student, Department of Mechanical Engineering. Member AIAA.

‡Research Scientist, Applied Aerodynamics Branch. Member AIAA.